

Fig. 1. Comparison of streamflow simulation results for the Heihe River Basin, northwestern China. Numerical models are effective approaches to simulate and analyze

streamflow rates were used to calibrate/train and verify the different methods. The root mean square error (RMSE) and the coefficient of determination (R^2) were used to evaluate the accuracy of the simulation/training and verification results.

The results showed that the accuracy of machine learning models was significantly better than that of numerical model in both stages. The SVM and RBF performed the best in training and verification stages, respectively. However, it should be noted that the generalization ability of numerical model is

poor. The RMSE and R^2 values for the numerical model in the training and verification stages are 1.2 and 0.8, respectively. The RMSE and R^2 values for the SVM and RBF models in the training and verification stages are 0.8 and 0.9, respectively.

streamflow rates were used to calibrate/train and verify the different methods. The root mean square error (RMSE) and the coefficient of determination (R^2) were used to evaluate the accuracy of the simulation/training and verification results.

With the rapid development of information science and technology, groundwater models have been widely used in exploration of groundwater dynamics, quantitative assessment of groundwater resources^{1,2}. A wide variety of models have been developed and applied for simulating groundwater dynamics which can be characterized as numerical (physical descriptive models) and empirical models. A major disadvantage of empirical models is the insufficient capability when confronting the dynamical behavior of the groundwater system changes. Many physically based numerical models for simulating groundwater system have been developed over the last 30 years^{3–8}. Unfortunately, the numerical models have their own limitations such as requiring a large quantity of accurate data which can never be ascertained with absolute accuracy (e.g., the physical properties of aquifer). Furthermore, the computation resources can hardly satisfy the increasing refinement and complexity of numerical models. In recent years, machine learning methods (e.g., Artificial Neural Networks (ANNs)⁹, Support Vector Machine (SVM)¹⁰) have been used for forecasting in hydrologic research domains. Carlos *et al.* applied random forest algorithm to spatially predict the water retention of soils and achieved good performance on predicting volumetric water contents¹¹. Gradient boosting¹² is a dominant learning method for the Classification and Regression Tree (CART). Gradient Boosting Decision Tree (GBDT) has been successfully applied in various prediction problems¹³. Kenda *et al.* presented a research applying data-driven modeling methods (Regression Trees, Random Forests and Gradient Boosting) to predict groundwater level changes with sufficiently well performance using data collected in Ljubljana aquifer¹⁴. A model based on machine learning for predicting timely stream flow data was developed and tested in Idaho and Washington in four diverse watersheds with highly accurate and reliable

¹China University of Petroleum-Beijing, College of Information Science and Engineering, Beijing, 102249, China.

²China University of Petroleum-Beijing, State Key Laboratory of Petroleum Resources and Prospecting, Beijing, 102249, China. ³CNPC Research Institute of Safety and Environmental Technology, Beijing, 102206, China. *email: chenchong@cup.edu.cn

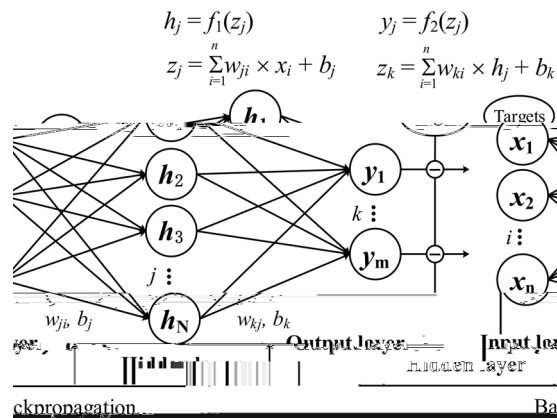


Figure 1. Schematic diagram demonstrating the architecture of backpropagation neural network. x_i , h_j and y_k represent the nodal values in the input layer, hidden layer and output layer, respectively; n , N and m are the number of nodes in the input layer, hidden layer and output layer; w_{ji} is the weight connecting the input x_i and the j th neuron in the hidden layer; w_{kj} is the weight connecting the j th neuron in the hidden layer (h_j) and the output y_k ; b_j and b_k are the biases in the hidden layer and output layer; f_1 and f_2 are the activation functions in the hidden layer and the output layer.

predictions compared to the recorded data¹⁵. A method was proposed by combining Extreme Learning Machine and Quantum-Behaved Particle Swarm Optimization and assessed with daily runoff data of Xinfengjiang reservoir in China¹⁶. Worland *et al.* compared the ability of eight machine learning models and four baseline models to estimate the annual minimum 7-day mean stream flow in ungagged basins and concluded that machine learning methods can produce more accurate predictions in ungagged basins than baseline models¹⁷. Taormina *et al.* presented a research of applying Forward Neural Networks (FNNs) for long term simulations of groundwater levels in a coastal unconfined aquifer and suggested to regard FNNs as an alternative for numerical models¹⁸. The main advantage of this approach is that it does not require the complex nature of the underlying process of the physical systems as in numerical models.

Groundwater plays a significant role as sources of supply for domestic, industrial and agricultural purposes. Groundwater resources have been overexploited in many parts of the world¹⁹, especially in arid and semi-arid regions with highly variable precipitation and considerably high evapotranspiration. The depleted groundwater resources lead to environmental side effects including groundwater level declines, drying up of wells, increased pumping costs, land subsidence, decreased well yields, reduction of water in streams and lakes and water quality degradation^{20,21}. Furthermore, population growth and climate extremes have significant influence on the quality and quantity of groundwater resources. Therefore, it is very important to sustainably manage groundwater resources in conjunction with surface water resources. Peng *et al.* analyzed the effects of water sources management strategies on water balance in North China and found reduced agriculture water consumption and sustained groundwater levels due to the decreased irrigation water use²². Sadeghi-Tabas *et al.* presented an attempt to link the multi-algorithm genetically adaptive search method (AMALGAM) with a numerical model to manage groundwater resources and found that “modeling - optimization - simulation” procedure was capable to obtain a set of optimal solutions²³. For the effective management of groundwater resources, it is of great significance to simulate the groundwater dynamics accurately and reliably. Accurate assessments of groundwater levels allow water managers, engineers, and stakeholders to develop better strategies for groundwater management and balance the needs of urban, agricultural, industrial and other demands and analyze the benefits and costs of water conservation.

In this study, a physically based numerical model (MODFLOW, Modular three-dimensional Finite-difference Ground-water Flow Model) and three machine learning methods were applied to simulate the groundwater dynamics of the middle reaches of Heihe River Basin, northwestern China. Collected data from 1986 to 2010 were divided into calibration/training and verification periods. The same data were used to calibrate/train different models. The objectives of our work are: (1) to explore the effectiveness of machine learning methods on simulating groundwater dynamics in arid basins; (2) to explore the applicability of machine learning methods and numerical models by comparing their results. The remainder of this paper is organized as follows: Section 2 presents methodologies for simulating the groundwater dynamics. Section 3 describes the study sites, the involved data and the processing of the data. The model structures, settings, hyperparameters and model performance criteria are presented in Section 4. Section 5 and 6 present the results, discussions and conclusions.

ANNs are mathematical structure inspired by the biological neural networks proposed by McCulloch²⁴. Multi-layer perceptron (MLP) is a class of feedforward ANN with input/output layers and several hidden layers. Nonlinear activation functions are used in the neurons to extract, learn and remember the nonlinear features and sub features from the inputs. Backpropagation is a family of methods which is always used to update the parameters in the ANN by calculating the gradient of a loss function with respect to all the

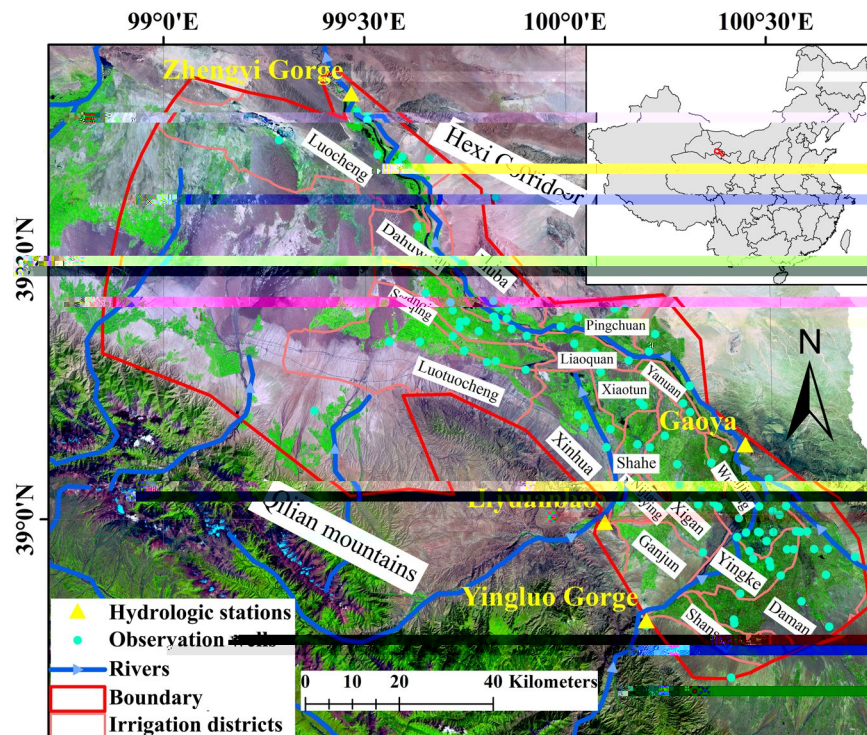


Figure 2. Map of the middle reaches of the Heihe River Basin. (Note: the map was generated using ESRI's ArcGIS 10.2 (<http://desktop.arcgis.com/en/arcmap/>); the satellite imagery was provided by Cold and Arid Regions Sciences Data Center at Lanzhou (<http://westdc.westgis.ac.cn>).

$$-K_n \frac{\partial h}{\partial n} \Big|_2 = q(x, y, z, t) \quad x, y, z \in \Omega_2, \quad t \geq 0 \quad (9)$$

Where K_x , K_y , and K_z are values of hydraulic conductivity along the x , y , and z coordinate axes ($L \cdot T^{-1}$); h is the hydraulic head (L) which can be converted to groundwater level; W represents source and/or sink term of water ($1/T$) with $W < 0.0$ for flowing out of the groundwater system, and $W > 0.0$ for flowing into the system; S_s denotes the specific storage of the aquifer ($1/L$); t is time (T); h_0 is the initial hydraulic head (L); Ω_2 denotes the study area; n is normal direction of a hydraulic boundary; Ω_1 denotes the top boundary condition of the study area; Ω_1 and Ω_2 are the Dirichlet boundary condition and Neumann boundary condition; and $q(x, y, z, t)$ is the normal discharge per unit width ($L^2(d \cdot L)^{-1}$). Solution of the groundwater flow equation is achieved by finite-difference method in which the groundwater flow system and simulation time are discretized into grids and stress periods, respectively. Each stress period is a period of simulation within which specified stress data are constant.

The Heihe River Basin which located in the middle of Qilian Mountain is the second largest inland river basin in the northwest of China. The basin extends ~821 km with an area of $\sim 14 \times 10^4$ km². The middle reaches of the Heihe River Basin (38°38'N–39°53', 98°53'E–100°44'E; Fig. 2) with an area of ~9016 km² was selected as the study area. The groundwater resource in this area has been overexploited for agricultural, industrial, and domestic use. The water system of the Heihe River Basin is composed of 35 independent rivers among which most of the mountainous rivers dry up because of irrigation water withdrawal and recharging to the aquifer in front of the mountains. The major rivers in the study area are the mainstream of the Heihe River and the Liyuan River. The Heihe River flows in the study area through the Yingluo Gorge hydrologic station and flows out of the study area through the Zhengyi Gorge hydrologic station (Fig. 2).

Various kinds of data including Digital Elevation Model (DEM), land use data, groundwater pumping yields, groundwater levels, stream flow rates, etc., were used in this study. All the available data were used to construct the numerical model; however, only time-variant data (i.e., stream flow rates, groundwater pumping rates, agricultural irrigation, and groundwater levels) were used to establish the machine learning models. Land use data were obtained through visual interpretation of Landsat TM/ETM+ images in 1986³⁴, 2000³⁵ and 2007³⁶. Historical data of groundwater levels from 42 monitoring wells (light blue dots in Fig. 2) were collected by the Gansu Provincial Bureau of Hydrology and were used in the study. The irrigation data were obtained from annual water resource management reports published by the Zhangye Municipal Bureau of Water Conservancy. Annual runoff at Yingluo, Gaoya and Zhengyi hydrologic stations (yellow triangle in Fig. 2) were collected from the Gansu Provincial Bureau of Hydrology. The data of groundwater exploitation during the modeling period were

obtained from China Census for Water. All the above-mentioned data were obtained from the “China Western Environment and Ecology Science Data Center” (<http://westdc.westgis.ac.cn>).

Elevation, irrigation, streamflow rates and pumping yields were processed to drive the numerical model. The elevation of the surface and bottom of the study area was obtained from the DEM which provided by the CGIAR-CSI GeoPortal. The resolution of the elevation was processed to 1 km from 90 m. Time-variant data were transformed into monthly stress periods (time interval) from January 1986 to December 2010. The calibration and verification periods were chosen as 1986–2008 and 2009–2010 because of the availability of relatively complete historical records. The main channels, tributaries and the divisions of the Heihe River were implemented using the Stream flow-Routing (STR) package³⁷. The stream flow rates measured at the Yingluo Gorge hydraulic station and Liyuan River were assigned to the STR package to simulate the rivers. Basic parameters (Stream state, top elevation of the streambed, bottom elevation of the streambed, width of the stream channel) were derived from³⁸. The agricultural irrigation was implemented using Recharge (RCH) package³ which combined the surface water and groundwater irrigation. The groundwater exploitation was simulated using the Well package³ by assigning pumping rates which were calculated from the extraction records.

Only time-variant data including stream flow rates, groundwater pumping rates, agricultural irrigation, and groundwater levels were used to construct the machine learning models. The time-series dataset was divided into two parts in accordance with the two stages in the numerical model building process: training and testing.

The training and testing periods were 1986–2008 and 2009–2010, respectively. The input and output data were summarized in Table 1 from which we could find existence of different units and ranges which would have influence on the results. Therefore, a normalization procedure was conducted for the machine learning methods to nondimensionalize the data to eliminate the effects of dimension as shown in Eq. (10). The data were normalized to the range of (−1, 1) after the procedure.

$$x^* = \frac{(y_{\max} - y_{\min}) \times (x - x_{\min})}{x_{\max} - x_{\min}} + y_{\min} \quad (10)$$

Where x is the original data; x^* represents the data after nondimensionalizing; x_{\min} and x_{\max} are the minimum and maximum value of x ; y_{\min} and y_{\max} are the lower and upper bound of the normalized data.

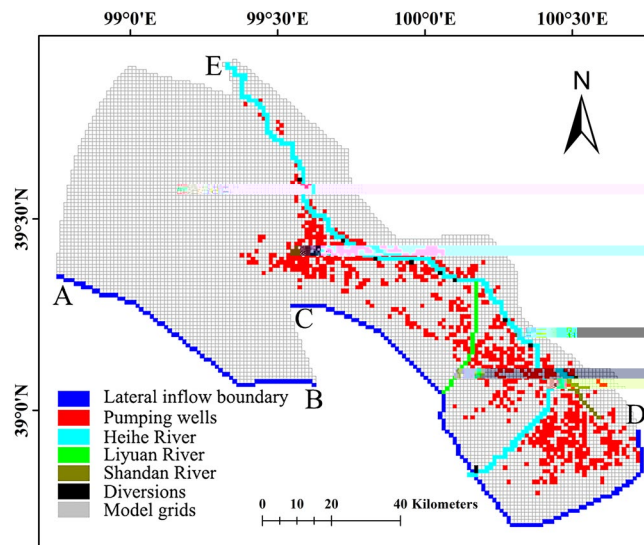


Figure 3. The numerical discretization and boundary conditions for the middle reaches of the Heihe River Basin.

All the machine learning methods were carried out in MATLAB 2017a environment running on a Intel Core i5, 2.5 GHZ CPU with DDR3L, 1600MHz RAM. The number of input layer neurons and output layer neurons were set based on the dimension of the input data and output data. The dimensions of input data include pumping rates and recharge rates of 21 irrigation districts (light red polygon in Fig. 2) and stream flow rates of two rivers (blue polyline in Fig. 2). The dimensions of the output data include groundwater levels observed at 42 boreholes (light blue dots in Fig. 2) and stream flow rates from two hydrologic stations (yellow triangle in Fig. 2). Therefore, the number of neurons in the input layer and output layer were both 44. As for the MLP, the hyperbolic tangent sigmoid transfer function and linear transfer function were applied in the neurons of the hidden layer and output layer, respectively. The number of hidden neurons was identified by trial and error procedure which started with two hidden neurons initially and increased to 10 with a step size of 1 at each trial. For each set of hidden neurons, the network was trained to minimize the Mean Square Error (MSE) at the output layer. Levenberg-Marquardt algorithm was used to update the values of weights and biases. The training was stopped when there was no significant improvement in the performance. The parsimonious structure that resulted in minimum error and maximum efficiency during training was selected as the final form of MLP. As for the RBF network, the Gaussian radial basis function and linear transfer function were applied in the neurons of the hidden layer and output layer, respectively. The number of hidden neurons was also identified by trial and error procedure which started with two hidden neurons and increased to 70. For each set of hidden neurons, the worst performing vector is added to the hidden layer as a Gaussian transfer function center to improve performance. Then the linear transfer function in the output layer was readjusted to minimize the MSE. As for the SVM, Gaussian function (also called radial basis function) was used as kernel function to compute the Gram matrix. Sequential minimal optimization (SMO)⁴⁴ was used to solve Eqs. (3) and (4). The output of SVM regression predictor was a one-dimensional vector. Therefore, 44 SVM regression models were trained using all 44-input data for each output vector. After training the machine learning methods, the machine learning models (MLP model, RBF model and SVM model) were generated for the study area.

As recommended by⁴⁵, the Root Mean Square Error (RMSE) and Coefficient of Determination (R^2) were used as objective functions to assess the groundwater level simulations through the calibration (training), verification (testing) stages (as shown in Eqs. (11) and (12)). The RMSE measures the average magnitude of the error between model simulations (M) and observations (O). As shown in Eq. (13), the errors are squared before averaged, large errors take a relatively high weight. Therefore, RMSE is useful when large errors are undesirable and R^2 measures the predictive ability of models.

$$RMSE = \sqrt{\frac{1}{N} \sum_{i=1}^N (M_i - O_i)^2} \quad (11)$$

$$R^2 = 1 - \frac{\sum_{i=1}^N (O_i - M_i)^2}{\sum_{i=1}^N (O_i - \bar{O})^2} \quad (12)$$

Where N represents the total number of observations; \bar{O} is the average of observations.

In the development of data-driven models (e.g., MLP, RBF, SVM), the most important issue is to guarantee the generalization ability of the models. Therefore, the generalization ability (GA) is evaluated as follows.⁴⁶

$$GA = \frac{RMSE \text{ in prediction stage}}{RMSE \text{ in training stage}} \quad (13)$$

The GA values are unity if the models simulate the groundwater system perfectly. However, if the models are over calibrated/trained, the GA values exceed unity. GA values less than unity indicates that the model is under calibrated/trained.

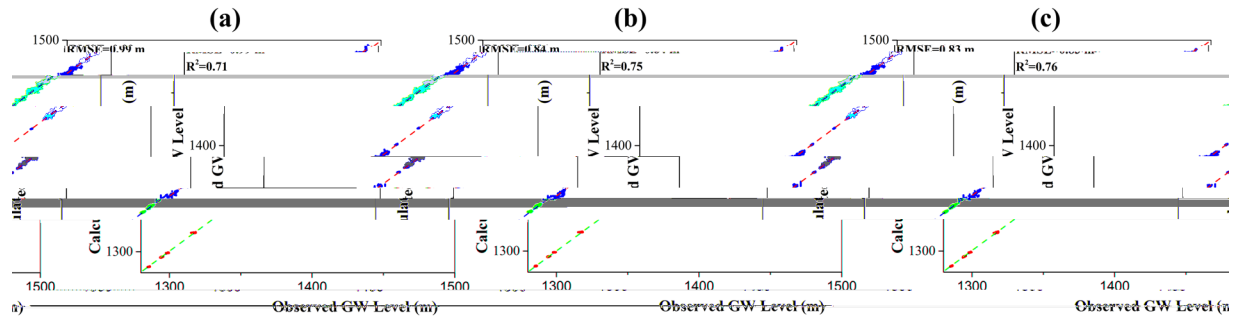


Figure 5. Comparison of the observed and simulated groundwater level for (a) MLP model; (b) RBF model; and (c) SVM model. Blue dots refer to the scatter plot of the observed and simulated groundwater level, the red dashed line denotes a perfect match where “simulated groundwater level = observed groundwater level”.

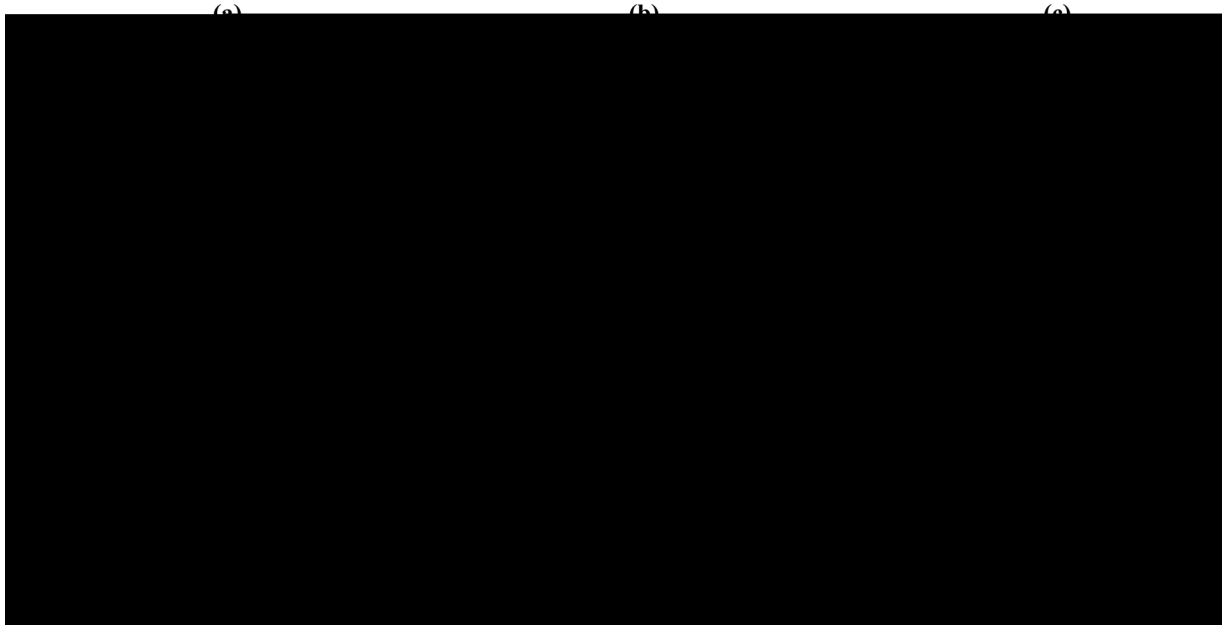


Figure 6. Comparison of the observed and simulated stream flow rates at Gaoya (*upper*) and Zhengyi (*lower*) Gorge hydraulic stations for (a) MLP model; (b) RBF model; and (c) SVM model. The blue curve refers to the simulated stream flow rates, the red dashed curve denotes the observed stream flow rates.

period. The comparison between observed and simulated groundwater levels and stream flow rates are shown in Fig. 7(a,b), respectively. The RMSE value and R^2 value for the groundwater levels are 5.84 m and 0.51, respectively.

The calculated stream flow rates of Gaoya and Zhengyi Gorge hydrologic stations shown in Fig. 7(b) match the observed stream flow rates considerably. Inspection of the comparison between calculated and observed groundwater levels and stream flow rates during the calibration and verification periods elucidates that the assumptions of boundary conditions made for the study area are appropriate and the establishment of the groundwater model for the middle reaches of the Heihe River Basin is feasible.

Figure 8 shows the comparison the observed and simulated groundwater levels for machine learning models in verification period. The models trained in the training stage were used to predict by applying new input data.

The RMSE and R^2 values were calculated using the model outputs and new observations. The RMSE and R^2 values are 1.69 m and 0.66, 1.12 m and 0.71, 1.71 m and 0.65 for MLP, RBF, and SVM models, respectively. The stream-flow rates predicted by machine learning models are shown in Fig. 9. The RMSE value and R^2 value for MLP, RBF, and SVM models calculated from stream flow rates at Gaoya and Zhengyi Gorge hydrologic stations are 1.69×10^6 m³/day and 0.54, 1.21×10^6 m³/day and 0.79, 1.17×10^6 m³/day and 0.83. In the verification period, the model based on RBF network performs the best. This may be due to the local transfer function and relatively large number of neurons in the hidden layer. The ANN methods (MLP and RBF network) are always based on an assumption of unlimited samples which can never be satisfied. The origin of SVM is based on limited samples and follows the structural risk minimization which adequately balanced the accuracy and generalization ability. SVM maps the input vectors into high-dimensional feature space by support vector and manage the problem following the linear optimization algorithm which avoids local minimum and Curse of Dimensionality.

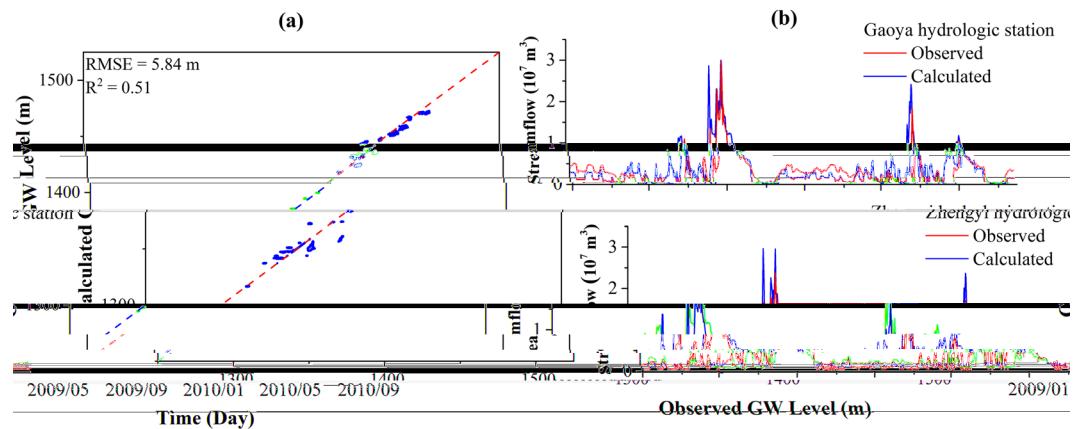


Figure 7. (a) Comparison of the observed and simulated groundwater level in verification period. Blue dots refer to the scatter plot of the observed and simulated groundwater level, the red dashed line denotes a perfect match where “simulated groundwater level = observed groundwater level”; (b) Comparison of the observed and simulated stream flow rates at Gaoya (upper) and Zhengyi (lower) Gorge hydraulic stations in verification period.

Generalization ability. The generalization ability was evaluated by Eq. (13) which indicates that GA values are greater if the model concentrates on learning the given training data rather than a more general system and that the higher the index values are, the weaker the generalization ability becomes. GA values (Table 2) calculated from groundwater level for MLP, RBF, and SVM models are 1.7, 1.3, and 2.1 which implies that the generalization ability of the RBF model is superior to that of MLP and SVM models. GA values calculated from stream flow rates for MLP, RBF, and SVM models are 1.55, 1.04, and 1.00. The overall values of GA which averages the two values of indices are 1.63, 1.18, and 1.53 which indicates that the generalization ability of RBF model is the lowest. Similar to the machine learning models, the generalization ability of numerical model was also evaluated by calculating GA values. The GA values calculated from groundwater level and stream flow rates for numerical model are 1.04 and 1.11 with the average of 1.08.

The comparison of numerical model and machine learning models in the calibration/training stage was conducted and shown in Table 3. RMSE and R^2 values were used to evaluate the accuracy of the simulated groundwater levels and stream flow rates compared to the observations. In this study, the RMSE and R^2 values imply that the accuracy of machine learning models is better than that of numerical model for the given data. Furthermore, the time elapsed in constructing the model is divided into two parts which are calibration/training time and computation time. The calibration of numerical model usually costs the hydrologist months to balance lots of aspects, processes and parameters. However, the machine learning methods only cost experts' days to determine the hyperparameters after data preparation. This is also the main reason why the calibration of the models is described in detail. Among the machine learning methods, the reproduction capability of groundwater levels and stream flow rates of RBF network and SVM is superior to that of MLP which may be caused by different transfer functions, network structures, and minimizing methods. The comparison between numerical model and machine learning methods in the verification/prediction stage is shown in Table 4. The performance of RBF model is better than that of numerical model, MLP model, and SVM model which indicates that RBF network is applicable to simulate groundwater systems. The comparison of generalization ability between different models is shown in Fig. 10. The generalization ability of numerical model calculated from groundwater levels is better than those of machine learning methods. The generalization ability of SVM model calculated from stream flow rates performs the best among all the models. It is noted that the overall generalization ability of the numerical model is superior to those of machine learning methods with lower generalization ability index value. The relatively less difference of generalization ability calculated from groundwater levels and stream flow rates indicates the stability of the numerical models. On the one hand, the RMSE value in calibration stage of numerical model which act as denominator in Eq. (13) is relatively large. On the other hand, the dynamics simulated by numerical model are based on the groundwater flow equation (Eq. (5)) with the same boundary conditions and parameters which dominates the groundwater movements. On the contrary, the machine learning methods are mappings between the inputs and outputs based on statistics without deduction of physical process. In the machine learning methods, the RBF model performs the best in generalization ability which is also close to the numerical model.

In this paper, the groundwater dynamics in the middle reaches of Heihe River Basin were simulated by numerical models and machine learning methods. Historical data of groundwater levels and stream flow rates were used to calibrate/train and verify/test the models. The RMSE and R^2 values were used to evaluate the simulated results of the constructed model which indicated that the calibrated model could considerably reproduce the trend and values of historical observations. Furthermore, a comparison was conducted to discover pros and cons of different models. The results showed that the performances of machine learning models on simulating historical data was superior to those of numerical model with RBF model performed the best. The computation cost of

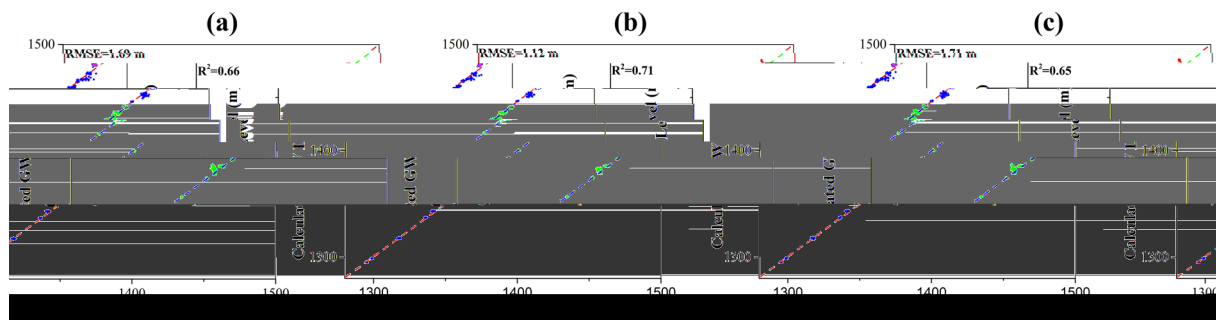


Figure 8. Comparison of the observed and simulated groundwater levels for (a) MLP model; (b) RBF model; (c) SVM model. Blue dots refer to the scatter plot of the observed and simulated groundwater level, the red dashed line denotes a perfect match where “simulated groundwater level = observed groundwater level”.

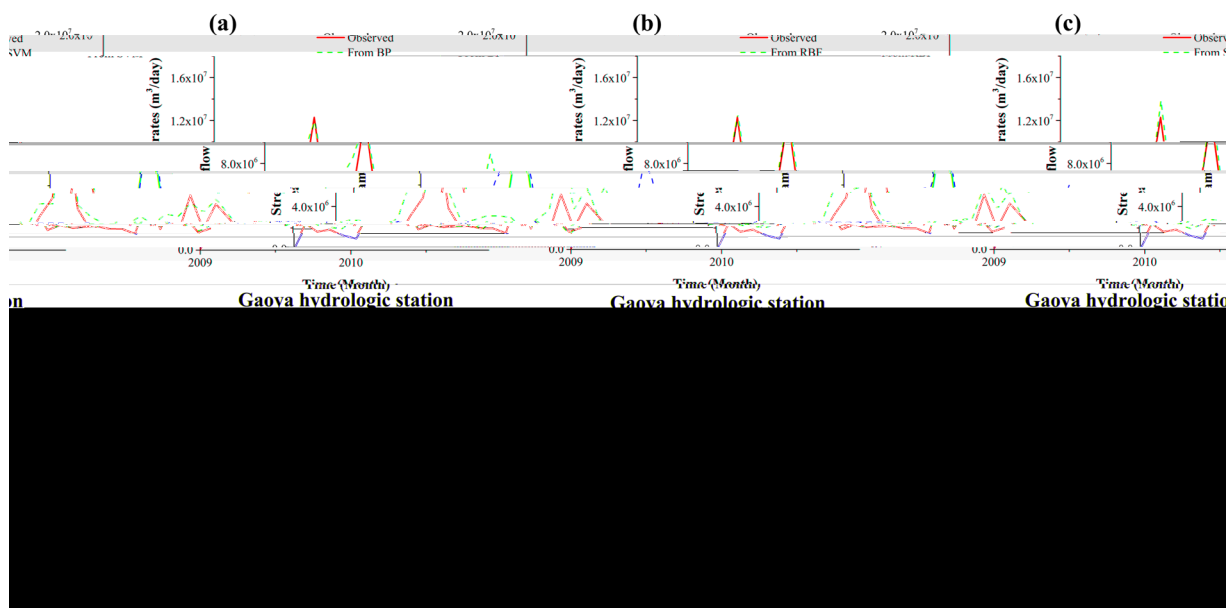


Figure 9. Comparison of the observed and simulated stream flow rates at Gaoya (*upper*) and Zhengyi Gorge (*lower*) hydraulic stations for (a) MLP model; (b) RBF model; (c) SVM model. The blue curve refers to the simulated stream flow rates, the red dashed curve denotes the observed stream flow rates.

	Numerical model	MLP model	RBF model	SVM model
Groundwater level	1.04	1.70	1.33	2.06
Stream flow rates	1.11	1.55	1.04	1.00
Overall	1.08	1.63	1.18	1.53

Table 2. Comparison of generalization ability.

		Numerical model	MLP model	RBF model	SVM model
RMSE	Groundwater level (m)	5.61	0.99	0.84	0.83
	Stream flow rates (m ³)	1.76 × 10 ⁶	1.09 × 10 ⁶	1.16 × 10 ⁶	1.16 × 10 ⁶
R ²	Groundwater level	0.52	0.71	0.75	0.76
	Stream flow rates	0.51	0.66	0.66	0.66
Time	Calibration	months	days	days	days
	Computation	1898 s	716.9 s	4.2 s	1.0 s

Table 3. Comparison in the calibration/training stage.

		Numerical model	MLP model	RBF model	SVM model
RMSE	Groundwater level (m)	5.84	1.69	1.12	1.71
	Stream flow rates (m ³)	2.05×10^6	1.69×10^6	1.21×10^6	1.17×10^6
R ²	Groundwater level	0.51	0.66	0.71	0.65
	Stream flow rates	0.50	0.54	0.79	0.83
	Time (s)	30	0.07	0.06	0.10

Table 4. Comparison in the verification stage.

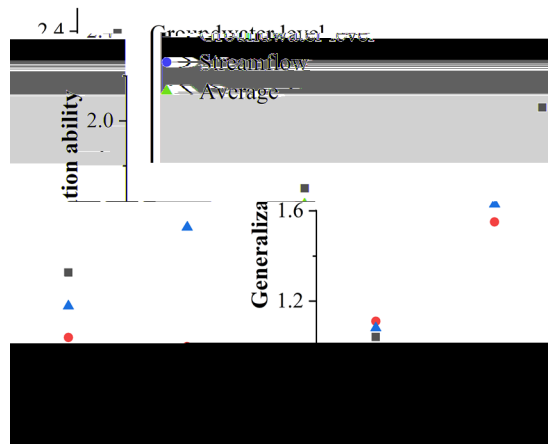


Figure 10. Comparison of generalization ability between different models.

machine learning models in training and prediction stages were much less than those of numerical model in calibration and verification stages. However, the generalization ability of the numerical model was better than that of machine learning methods because of the physical based mechanism. Therefore, machine learning models are applicable to the scenarios which require numerous executions without considering the physical mechanisms (e.g., real-time models, sensitivity/uncertainty analysis, and optimizations). The developed models and the results of this study may be useful for the accurate groundwater management, decision making, and model selection. Future research should be focused on exploring applicability of deep learning methods or tree-based machine learning algorithms in hydrologic field and application of the developed models to manage groundwater resources.

Received: 22 November 2018; Accepted: 7 February 2020;

Published online: 03 March 2020

- Loucks, D. P., Kindler, J. & Fedra, K. Interactive Water Resources Modeling and Model Use: An Overview. *Water Resour. Res.* **21**, 95–102, <https://doi.org/10.1029/WR021i002p00095> (1985).
- Singh, A. Groundwater resources management through the applications of simulation modeling: A review. *SciEn* **499**, 414–423, <https://doi.org/10.1016/j.scitotenv.2014.05.048> (2014).
- Harbaugh, A. W. MODFLOW-2005: The US Geological Survey modular ground-water model—The ground-water flow process. Report No. 6-A16, (U.S. Geol. Surv., Tech. Methods 2005).
- Markstrom, S. L., Niswonger, R. G., Regan, R. S., Prudic, D. E. & Barlow, P. M. GSFLOW - Coupled Ground-Water and Surface-Water Flow Model Based on the Integration of the Precipitation-Runoff Modeling System (PRMS) and the Modular Ground-Water Flow Model (MODFLOW-2005). Report No. 6-D1, 240 (2008).
- Neitsch, S. L., Arnold, J. G., Kiniry, J. R. & Williams, J. R. Soil and water assessment tool theoretical documentation version 2009. (Texas Water Resources Institute 2011).
- Storm, B. & Høgh Jensen, K. Experience with field testings of SHE on research catchments. *Hydrol. Res.* **15**, 283–294, <https://doi.org/10.2166/nh.1984.0025> (1984).
- Diersch, H.-J. *FEFLOW: Finite Element Modeling of Flow, Mass and Heat Transport in Porous and Fractured Media*. (Springer-Verlag Berlin Heidelberg 2014).
- Boogaard, H. L., Diepen, C. A. v., Rotter, R. P., Cabrera, J. M. C. A. & Laar, H. H. v. WOFOST 7.1; user's guide for the WOFOST 7.1 crop growth simulation model and WOFOST Control Center 1.5. Report No. 0927-4499, (SC-DLO, Wageningen 1998).
- LeCun, Y., Bengio, Y. & Hinton, G. Deep learning. *Nature*. **521**, 436–444, <https://doi.org/10.1038/nature14539> (2015).
- Vapnik, V. *The Nature of Statistical Learning Theory*. (Springer science & business media 2013).
- Guio Blanco, C. M., Brito Gomez, V. M., Crespo, P. & Ließ, M. Spatial prediction of soil water retention in a Páramo landscape: Methodological insight into machine learning using random forest. *Geoderma*. **316**, 100–114, <https://doi.org/10.1016/j.geoderma.2017.12.002> (2018).
- Friedman, J. H. Greedy function approximation: A gradient boosting machine. *Ann. Stat.* **29**, 1189–1232, <https://doi.org/10.1214/aos/1013203451> (2001).

13. Fioren, M. N., Nolan, B. T., Kaufman, L. J. & Feinstein, D. T. Metamodeling for Groundwater Age Forecasting in the Lake Michigan Basin. *Water Resources Research* **54**, 4750–4766, <https://doi.org/10.1029/2017wr022387> (2018).
14. Kenda, K. *et al.* Groundwater modeling with machine learning techniques: Ljubljana polje Aquifer. *Proceedings* **2**, 697, <https://doi.org/10.3390/proceedings2110697> (2018).
15. Petty, T. R. & Dhingra, P. Stream flow hydrology estimate using machine learning (SHEM). *J. Am. Water Resour. Assoc.* **54**, 55–68, <https://doi.org/10.1111/1752-1688.12555> (2018).
16. Niu, W., Feng, Z., Cheng, C. & Zhou, J. Forecasting daily runoff by extreme learning machine based on quantum-behaved particle swarm optimization. *J. Hydrol. Eng.* **23**, 1–10, [https://doi.org/10.1061/\(ASCE\)HE.1943-5584.0001625](https://doi.org/10.1061/(ASCE)HE.1943-5584.0001625) (2018).
17. Worland, S. C., Farmer, W. H. & Kiang, J. E. Improving predictions of hydrological low-flow indices in ungaged basins using machine learning. *Environ. Modell. Softw.* **101**, 169–182, <https://doi.org/10.1016/j.envsoft.2017.12.021> (2018).
18. Taormina, R., Chau, K.-W. & Sethi, R. Artificial neural network simulation of hourly groundwater levels in a coastal aquifer system of the Venice lagoon. *Eng. Appl. of Artif. Intel.* **25**, 1670–1676, <https://doi.org/10.1016/j.engappai.2012.02.009> (2012).
19. Konikow, L. F. & Kendy, E. Groundwater depletion: A global problem. *Hydrogeol. J.* **13**, 317–320, <https://doi.org/10.1007/s10040-004-0411-8> (2005).
- 20.

The authors declare no competing interests.

Correspondence and requests for materials should be addressed to C.C.

Reprints and permissions information is available at www.nature.com/reprints.

Publisher's note Springer Nature remains neutral with regard to jurisdictional claims in published maps and institutional affiliations.



Open Access This article is licensed under a Creative Commons Attribution 4.0 International License, which permits use, sharing, adaptation, distribution and reproduction in any medium or format, as long as you give appropriate credit to the original author(s) and the source, provide a link to the Creative Commons license, and indicate if changes were made. The images or other third party material in this article are included in the article's Creative Commons license, unless indicated otherwise in a credit line to the material. If material is not included in the article's Creative Commons license and your intended use is not permitted by statutory regulation or exceeds the permitted use, you will need to obtain permission directly from the copyright holder. To view a copy of this license, visit <http://creativecommons.org/licenses/by/4.0/>.

© The Author(s) 2020